

Two Types of Martian Magnetotail Current Sheets: MAVEN Observations of Ion Composition

XinZhou Li¹, Zhaojin Rong¹, Markus Fraenz², Lucy Klinger³, Zhen Shi¹, Chi Zhang¹, Jiawei Gao¹, and Yong Wei¹

¹Institute of Geology and Geophysics Chinese Academy of Sciences

²Max Planck Institute for Solar System Research

³Beijing International Center for Mathematical Research

November 23, 2022

Abstract

The ion composition of the tail current sheet is essential to understanding the Martian ion escape, however, our current knowledge is poor. Using measurements by Mars Atmosphere and Volatile Evolution (MAVEN), we investigate the density of different ion species in the Martian magnetotail current sheet. We find that events we survey of the current sheet, the average occurrence rate of current sheets with dominant heavy ions (O⁺ and O₂⁺) is about 50%, while the rate of those with dominant H⁺ is about 20%. A current sheet closer to the terminator is mostly dominated by heavy ions, regardless of upstream solar wind, but it could be dominated sometimes by H⁺ when it is beyond the downstream distance of 0.75 RM (RM is Mars' radius), where the occurrence rate of current sheets with dominant H⁺ (heavy ions) weakly increases (decreases) with solar wind density and dynamic pressure.

Hosted file

supporting information for "two types of martian magnetotail current sheets maven observations of ion composition" available at <https://authorea.com/users/542502/articles/601988-two-types-of-martian-magnetotail-current-sheets-maven-observations-of-ion-composition>

Hosted file

essoar.10512369.1.docx available at <https://authorea.com/users/542502/articles/601988-two-types-of-martian-magnetotail-current-sheets-maven-observations-of-ion-composition>

Two Types of Martian Magnetotail Current Sheets: MAVEN Observations of Ion Composition

X. Z. Li^{1, 2}, Z. J. Rong^{1, 2, 3*}, Markus Fraenz⁴, L. Klinger⁵, Z. Shi^{1, 2}, C. Zhang^{1, 2},

J.W. Gao^{1, 2}, Y. Wei^{1, 2, 3}

¹Key Laboratory of Earth and Planetary Physics, Institute of Geology and Geophysics, Chinese Academy of Sciences, Beijing, China

²College of Earth Science, University of Chinese Academy of Sciences, Beijing, China

³Mohe Observatory of Geophysics, Institute of Geology and Geophysics, Chinese Academy of Sciences; Beijing, China.

⁴Max Planck Institute for Solar System Research, Göttingen, Germany

⁵Beijing International Center for Mathematical Research, Peking University, Beijing, China

Corresponding author: Z. J. Rong (rongzhaojin@mail.iggcas.ac.cn)

Key Points:

- Two types of Martian tail current sheets are classified according to their dominant ion species.
- Current sheets are mostly dominated by heavy ions when closer to the terminator and sometimes dominated by H⁺ when $X < -0.75 R_M$.
- The occurrence rate of current sheets with dominant H⁺/heavy ions weakly increases/decreases with solar wind density and dynamic pressure.

Abstract

The ion composition of the tail current sheet is essential to understanding the Martian ion escape, however, our current knowledge is poor. Using measurements by Mars Atmosphere and Volatile Evolution (MAVEN), we investigate the density of different ion species in the Martian magnetotail current sheet. We find that events we survey of the current sheet, the average occurrence rate of current sheets with dominant heavy ions (O⁺ and O₂⁺) is about 50%, while the rate of those with dominant H⁺ is about 20%. A current sheet closer to the terminator is mostly dominated by heavy ions, regardless of upstream solar wind, but it could be dominated sometimes by H⁺ when it is beyond the downstream distance of 0.75 R_M (R_M is Mars' radius), where the occurrence rate of current sheets with dominant H⁺ (heavy ions) weakly increases (decreases) with solar wind density and dynamic pressure.

Plain Language Summary

The current sheet of the Martian magnetotail is a major channel for the escape of planetary ions. The ion composition in the current sheet is essential to

understanding this escape as well as magnetotail plasma dynamics; our current knowledge, however, is poor. Based on the measurements of MAVEN regarding the ion density of different species in the current sheet, we report that the current sheets we survey are dominated by either the heavy ions from the planet or by the H^+ mostly from solar wind. We find that downstream distance and the variation of upstream solar wind are the two key factors that control the variation of dominant ion species in the tail current sheet.

1 Introduction

Unlike Earth, Mars does not possess an intrinsic global dipolar magnetic field, which leads to the direct interaction of the Martian ionosphere/atmosphere with solar wind and the scavenging of planetary ions (e.g., Luhmann and Brace, 1991, and references therein; Zhang et al., 2021). The “frozen-in” interplanetary magnetic field (IMF), carried by solar wind plasma flow, is draped around Mars as solar wind approaches the planet. This draped IMF would then slip into the wake, resulting in an elongated induced magnetotail that is characterized by a pair of the magnetic lobes with antiparallel field lines as well as a current sheet between the lobes (e.g., Fedorov et al., 2008; Dubinin and Fraenz, 2015; Zhang et al., 2022).

The Martian magnetotail plays an important role in controlling the distribution and escape of planetary ions (e.g., Liemohn and Xu, 2018, and references therein). Based on the spacecraft measurements by Mars Global Surveyor (Acuña et al., 1998), Mars Express (Barabash et al., 2006), Mars Atmosphere and Volatile EvolutioN (MAVEN) (Jakosky et al., 2015), as well as simulations and particle tests, the properties and dynamics of Martian tail have been widely surveyed and studied (e. g: Eastwood et al., 2008; Fedorov et al., 2008; Halekas et al. 2009; Harada et al., 2015; Brain et al., 2010; DiBraccio et al., 2015; Dubinin and Fraenz, 2015; Ma et al., 2015). Regarding Mars Express, for example, Barabash et al. (2007) demonstrated that planetary ions, including not only O^+ but also molecular ions such as O_2^+ and CO_2^+ , move down through the magnetotail. Carlsson et al. (2006) found that the most abundant species of the escaping ions from Martian tail was O^+ , followed by O_2^+ and CO_2^+ . Nilsson et al. (2010) conducted a survey of H^+ and O^+ fluxes by Mars Express and found out that the H^+ flux dramatically decreases inside the magnetospheric boundary and that the Martian tail is dominated by planetary ions. Based on a simulated density of H^+ and planetary ions, some researchers concluded that planetary ions dominate the whole tail region (Najib et al., 2011; Xu et al., 2016). Using MAVEN data, Inui et al., (2019) statistically investigated the outflows of heavy ions in the Martian wake by MAVEN and found an average density ratio of $O^+ : O_2^+ : CO_2^+$ (~29:68:04). DiBraccio et al.,(2015) studied an event of the tail current sheet and found the density of H^+ is much less than that of O_2^+ and O^+ in the sheet, however, the density of H^+ sometimes becomes comparable to that of O_2^+ and O^+ (Artemyev et al., 2017).

In the Martian magnetotail, the tail current sheet is a transition layer between lobes and thus a key channel for planetary ion escape. Because the draped field

lines over the current sheet are highly stretched, it is able to drive ions moving tailward due to its significant tailward $\mathbf{j} \times \mathbf{B}$ force (e.g., Dubinin and Fraenz, 2015; Liemohn and Xu, 2018, and references therein; Zhang et al., 2022). Therefore, the knowledge of ion composition is essential to understanding the escape of planetary ions in the tail current sheet and its plasma dynamics. However, few studies focus on the ion composition in the tail current sheet despite the observation that heavy ions from the ionosphere are dominant in the Martian tail [Liemohn and Xu, 2018, and references therein].

Here, based on the case studies and a statistical survey of MAVEN’s observations, we focus exclusively on the ion composition in the Martian tail current sheet and demonstrate, for the first time, that there are at least two types of tail current sheets: one dominated by H^+ and another dominated by planetary heavy ions (O^+ and O_2^+). Our findings significantly update current knowledge of plasma composition in the Martian tail and would benefit further studies on planetary ion escape through the tail.

The datasets and coordinates we use are introduced in section 2 and typical events are shown in section 3. In section 4, we conduct a statistical survey based on selected events. Finally, we discuss and summarize the results in section 5.

2 Dataset and Coordinates

The MAVEN spacecraft was launched on 18 November 2013 and began orbiting Mars on 21 September 2014 (Jakosky et al., 2015). This spacecraft, in primary science phase, had an elliptical orbit with an inclination 75° that lasted for a period of about 4.5 hours. Such an orbit can reach a periapsis altitude of ~ 150 km and an apoapsis altitude of $\sim 6,200$ km. MAVEN’s orbit, due to the orbit precession, can be sampled at all local times and covers the latitude range $-75^\circ \sim +75^\circ$.

The MAVEN datasets we used are derived from the measurements taken by the magnetometer (MAG, Connerney et al., 2015), the Solar Wind Ion Analyzer SWIA, Halekas et al., 2015, and the Supra-Thermal And Thermal Ion Composition (STATIC, McFadden et al., 2015). MAG can measure the magnetic field vector with a maximum resolution of 32Hz; in this study, however, the MAG dataset was processed with a resolution of 1 Hz. SWIA is an electrostatic analyzer designed to measure solar wind and magnetospheric ions over an energy range of ~ 5 -25000 eV/q and an angular range of $360^\circ \times 90^\circ$. STATIC is also an electrostatic analyzer, but with a $360^\circ \times 90^\circ$ field-of-view that is combined with a time-of-flight velocity analyzer, which is able to differentiate ion species within the energy range of 0.1 eV–30 keV. Different science data products of STATIC have been publicly released, and the L2 data set, labeled as “C6_32e64m,” is used to show the energy flux of ions because it offers a high resolution of ion spectrum with 32 energy levels and 64 mass arrays. In our study, we extract energy fluxes with $m/q < 1.2$ for H^+ and with $m/q > 10$ for heavy ions.

Meanwhile, by joining several L2 telemetry products of STATIC (c0, cf, d1, ce, d0, cd, cc, and ca) onto a grid of 32 energies, 4 polar angles, 16 anodes

and 8 masses at 4s resolution, we can derive the plasma moments (density, velocity, and temperature) of H^+ (mass channels 0–1), O^+ (mass channel 4), and O_2^+ (mass channel 5–6) respectively (see Dubinin et al.,2020). Initially, the products of these plasma moments were classified into two types according to their energy range coverage: that is, products covering 30eV–30keV (labeled with the subscript “_high”) and products covering 0–30eV (labeled with the subscript “_low”), where products of low-energy ions have been corrected for the spacecraft’s potential. Thus, for H^+ , density and bulk velocity are calculated as n_{H^+} and v_{H^+} . Density and bulk velocity for O^+ and O_2^+ can be calculated similarly.

Two coordinates are used in this study. The first is Mars-centered Solar Orbital (MSO) coordinates, where +X points sunward, +Z is perpendicular to Mars orbital plane and positive toward the ecliptic north, and +Y completes the right-handed system. The second is Mars-Solar-Electric field (MSE) coordinates, where +X points in the Sun direction ($X_{MSE}=X_{MSO}$), +Z points in the solar wind convection electric field direction ($Z_{MSE}=E_{SW}=-V_{SW}\times B_{IMF}$), and +Y completes the right-handed system ($Y_{MSE}=Z_{MSE}\times X_{MSE}$). Using the magnetic field dataset and the plasma velocity measured by the spacecraft upstream of solar wind, MSE coordinates corresponding to a given orbit can be derived.

3. Events of tail current sheets

Typical cases recorded by MAVEN are shown here to demonstrate the discrepancy of dominant ion species in the tail current sheet.

3.1. Event on 4 October 2016

In Figure 1, we show that two successive crossings of a tail current sheet occurred in one orbit on October 4, 2016. Obviously, in this event, MAVEN crossed the tail current sheet at 11:07 (crossing 1) and 11:29 (crossing 2) (see vertical dashed lines in Figure 1) when the spacecraft was at ($X_{MSO}=-0.61$, $Y_{MSO}=1.06$, $Z_{MSO}=0.53$) R_M and ($X_{MSO}=-1.20$, $Y_{MSO}=0.46$, $Z_{MSO}=1.35$) R_M ($R_M=3390$ km, Mars radius), respectively. The spacecraft recorded typical signatures of the tail current sheet: that the B_x component of the magnetic field in the tail reverses its polarity (Figure 1d) and the energy flux of ions is enhanced simultaneously (Figure 1e). By taking the average of the IMF and upstream solar wind velocity over 5~15 minutes before the inbound and after the outbound crossing of the bow shock, we find the average proton number density and speed of solar wind are 2.4 cm^{-3} and 369.7 km/s respectively, and the IMF in MSO is ($B_x=-0.54$, $B_y=1.55$, $B_z=1.25$) nT. Thus, at the two crossings, the corresponding spacecraft locations in MSE are estimated to be ($X_{MSE}=-0.61$, $Y_{MSE}=0.59$, $Z_{MSE}=-1.04$) R_M and ($X_{MSE}=-1.20$, $Y_{MSE}=1.38$, $Z_{MSE}=-0.37$) R_M .

Nonetheless, a comparison of ion species shows differences between the two crossings. For crossing 1, the energy flux of heavy ions with energy ~ 400 eV shows an enhancement that is higher than that of H^+ (Figure 1f-1g). The number density of either O^+ or O_2^+ is also higher than that of H^+ (Figure 1h); thus, heavy ions dominate the current sheet. The bulk velocities of H^+ , O^+ , and O_2^+ are tailward with comparable speeds during this crossing (Figure

1j). In contrast, for crossing 2, the energy flux of H^+ with energy ~ 400 eV shows an enhancement and is higher than that of heavy ions. Accordingly, the calculated density of H^+ is much higher than those of O^+ and O_2^+ ; thus, H^+ is the dominant ion in this sheet (Figure 1i), and the tailward velocity of H^+ is far greater than those of O^+ and O_2^+ (Figure 1k).

For concision, we denote a current sheet with a dominant ion H^+ as an “L-sheet” (i.e., a sheet with light ions) and one with dominant heavy ions (O^+ and O_2^+) as an “H-sheet” (i.e., a sheet with heavy ions).

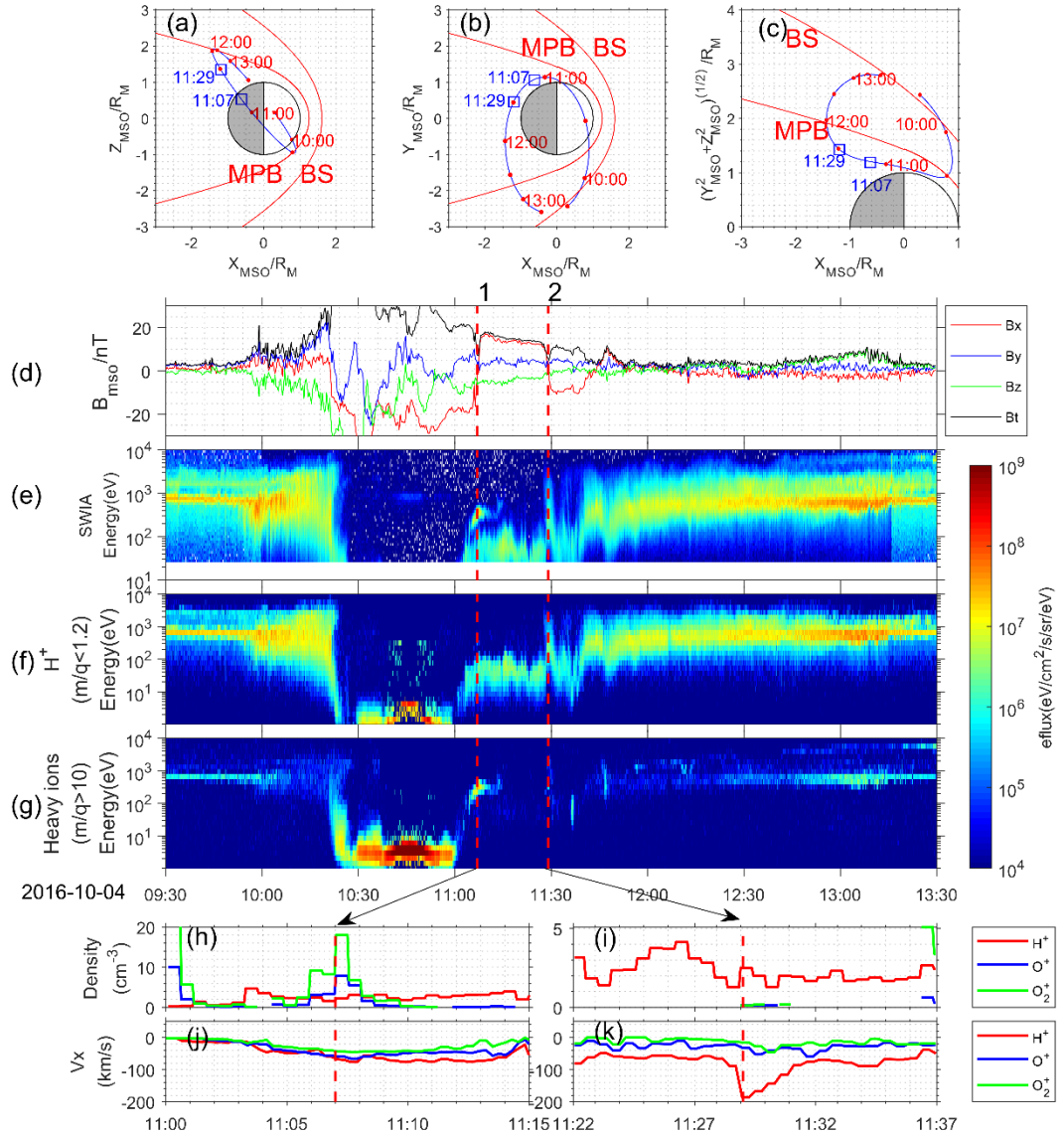


Figure 1. A typical event of crossing the Martian tail current sheet by MAVEN on October 4, 2016. From top to bottom, panels show the trajectory of the spacecraft in MSO coordinates (a, b); the time series of the magnetic field in MSO (c); the spectra of energy flux of ions (d), electrons (e), H^+ (f), and heavy ions (g); and the time series of number densities of H^+ , O^+ , and O_2^+ (h, i) and the x component of velocity of H^+ , O^+ , and O_2^+ (j, k). In panels (a) and (b), the average position of the magnetic pile-up boundary (MPB) and bow shock (BS), calculated by the model of Troignon et al. (2006), are shown in red curves.

The vertical dashed red lines mark crossings of the tail current sheet at 11:07 and 11:29.

3.2. Event on 19 December 2016 VS. Event on 10 April 2018

As shown in Figure 2 (left column), MAVEN recorded a tail current sheet crossing at 21:05 on 19 December 2016. The average solar wind proton number density and the speed for this orbit are 0.86 cm^{-3} and 626.7 km/s respectively, and the IMF in MSO is $(B_x=-1.06, B_y=-0.15, B_z=0.66) \text{ nT}$. At the moment of crossing, the spacecraft is located at $(X_{\text{MSO}}=-1.72, Y_{\text{MSO}}=0.06, Z_{\text{MSO}}=0.18) R_{\text{M}}$ in MSO or $(X_{\text{MSE}}=-1.72, Y_{\text{MSE}}=0.15, Z_{\text{MSE}}=0.13) R_{\text{M}}$ in MSE; here, the energy flux of H^+ shows an enhancement within the energy range 10–100 eV, which is higher than that of heavy ions (Figure 2c-2d). The number density of H^+ is much higher than that of O^+ or O_2^+ (Figure 2e). Thus, for this case, the current sheet is dominated by H^+ and can be classified as an L-sheet.

Nonetheless, for the current sheet crossing at 18:10 on 10 April 2018 (right column of Figure 2), MAVEN was located at $(X_{\text{MSO}}=-1.80, Y_{\text{MSO}}=-0.08, Z_{\text{MSO}}=0.16) R_{\text{M}}$, nearly the same downstream distance as in the case of 19 December 2016 (the left column of Figure 2). For this orbit, the average solar wind proton number density and the speed are 4.01 cm^{-3} and 383.6 km/s respectively, and the IMF in MSO is $(B_x=-0.03, B_y=2.74, B_z=-0.31) \text{ nT}$. The crossing location of the spacecraft in MSE is $(X_{\text{MSE}}=-1.80, Y_{\text{MSE}}=0.04, Z_{\text{MSE}}=0.17) R_{\text{M}}$. In this case, the energy flux of heavy ions (which is enhanced over the energy range of 10–100 eV) is higher than that of H^+ (Figure 2i-2j). The number densities of O^+ and O_2^+ are also much higher than that of H^+ (Figure 2k); thus, this current sheet is a type of H-sheet.

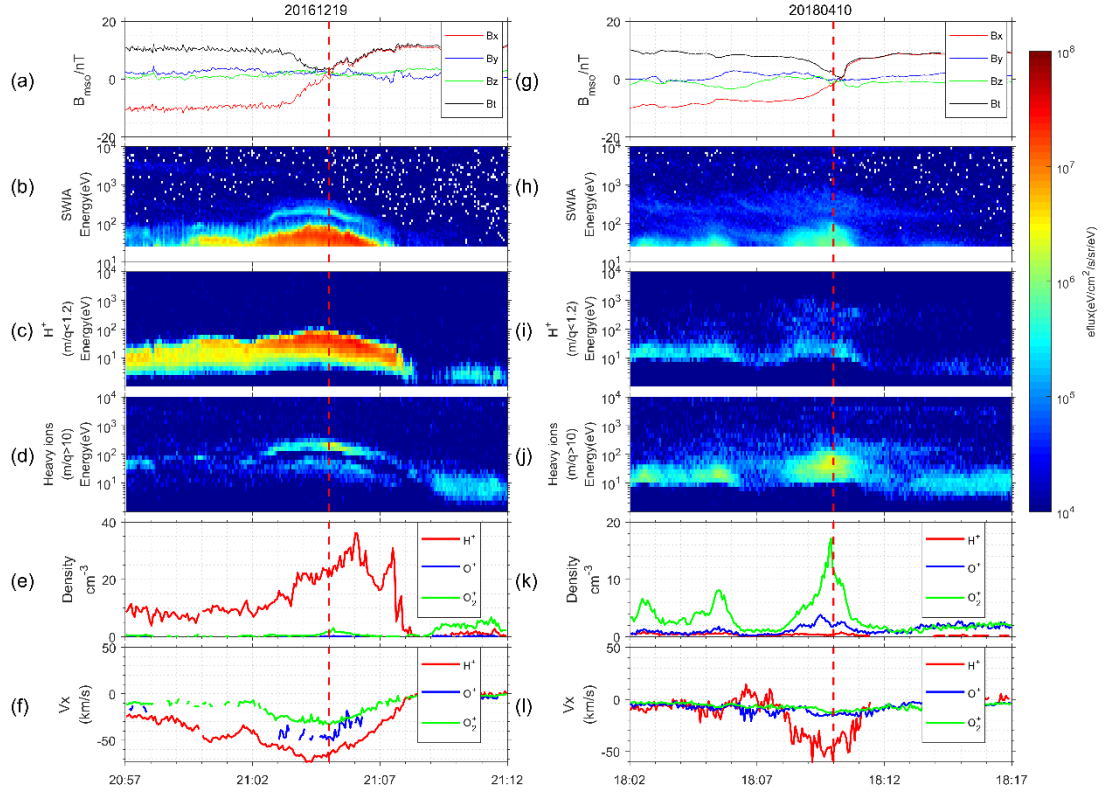


Figure 2. The crossing of the Martian tail current sheet by MAVEN on 19 December 2016 (left column) and on 10 April 2018 (right column). The format is the same as the one in Figure 1.

3.3 Summary of Events

Looking at the events recorded in Figure 1 and Figure 2, it is obvious that ion composition in the Martian tail current sheet is variable. The current sheet is dominated either by H^+ or, at times, heavy ions. However, the reasons for this are unclear.

For the event shown in subsection 3.1, the successive occurrence of an L-sheet and then an H-sheet within the short period of 22 minutes demonstrates that solar wind cannot be the sole factor that induces change in the dominant ion species, because the typical timescale of solar wind discontinuity, e.g. co-rotating interaction region, is much longer than 22 minutes (Verscharen et al., 2019). And, for this event, the speeds and densities of upstream solar wind for both inbound and outbound crossings of magnetosphere are nearly constant (not shown here). Thus, such ion variation might be caused by other factors including spatial ones, e.g., the downstream distance between crossing locations.

While the locations of both the L-sheet and the H-sheet, as shown in subsection 3.2, are almost identical in either MSO or MSE, variation of ion composition cannot be caused by changes in the spacecraft’s location, but may be associated with variability in external solar wind (note that solar wind has a faster speed and lower density for the case of L-sheet, and a lower speed and higher density for the case of H-sheet).

4 Statistical Study

To survey the factors in determining the dominant ion species in a Martian tail current sheet, we select and classify the crossing events of the tail current sheet, and study the occurrence rate of this current sheet, demonstrating statistically how each type varies according to downstream distance and to solar wind parameters.

4.1 Selection Criteria

From the time series of MAG data and the energy flux spectrum of SWIA from 11 October 2014 to 31 December 2020, we selected crossings of the Martian tail current sheet on the following criteria:

1. The spacecraft should be located within the magnetotail ($X_{\text{MSO}} < 0$). One can visually identify the tail’s boundary because its external magnetosheath has a continual spectrum of solar wind ions with energy typically larger than 800 eV and a highly fluctuated magnetic field (see Figure 1).
2. The energy flux of ions measured by SWIA shows an enhancement at the reversal of the B_x component.
3. To exclude the pseudo-crossings associated with crustal fields, the crossings must satisfy $B - B_c / B > 0.5$, where B is the measured magnetic field strength at the reversal of B_x , and B_c is the crustal field strength estimated by the model of Gao et al. (2021).

We selected a total of 1426 crossing cases. To classify the current sheet according to the dominant ion species, we average the number densities of H^+ , O^+ , and O_2^+ within the period $B_x < 5$ nT respectively. We define that if the average number density of H^+ is twice the sum of O^+ and O_2^+ , that is, , the current sheet is denominated as H^+ and is an L-sheet. Similarly, a sheet is dominated by heavy ions if and is classified as an H-sheet. From our 1426 cases, we found 331 L-sheets, 678 H-sheets, and 417 with no obvious classification (see Figure S1a-S1b in Supporting Information S1). Thus, on average, the occurrence rate is about 20% for L-sheets and about 50% for H-sheets.

4.2 Statistical Distributions

From the selected cases above, we select cases whose solar wind measurements

are available in corresponding orbits to survey possible correlations between the occurrence of the current sheet of a given type and the upstream solar wind. Here, 844 crossing cases were found: 191 L-sheet crossings and 397 H-sheet crossings.

The spatial distributions of these events demonstrate that both types of current sheet can occur widely in the Martian tail (Figure 3a and Figure S1a in Supporting Information S1) and that this sheet dominated by a H-sheet when closer to the terminator ($X > -0.75 R_M$). The occurrence rate shown in Figure 3b-3c is defined as the ratio of the current sheet number of a given type to the total current sheet number in a bin. The occurrence rate suggests that, apart from the dominance of the H-sheet closer to the terminator, both types of the sheet can appear beyond $X < -0.75 R_M$ at a significant rate (Figure 3b-3c).

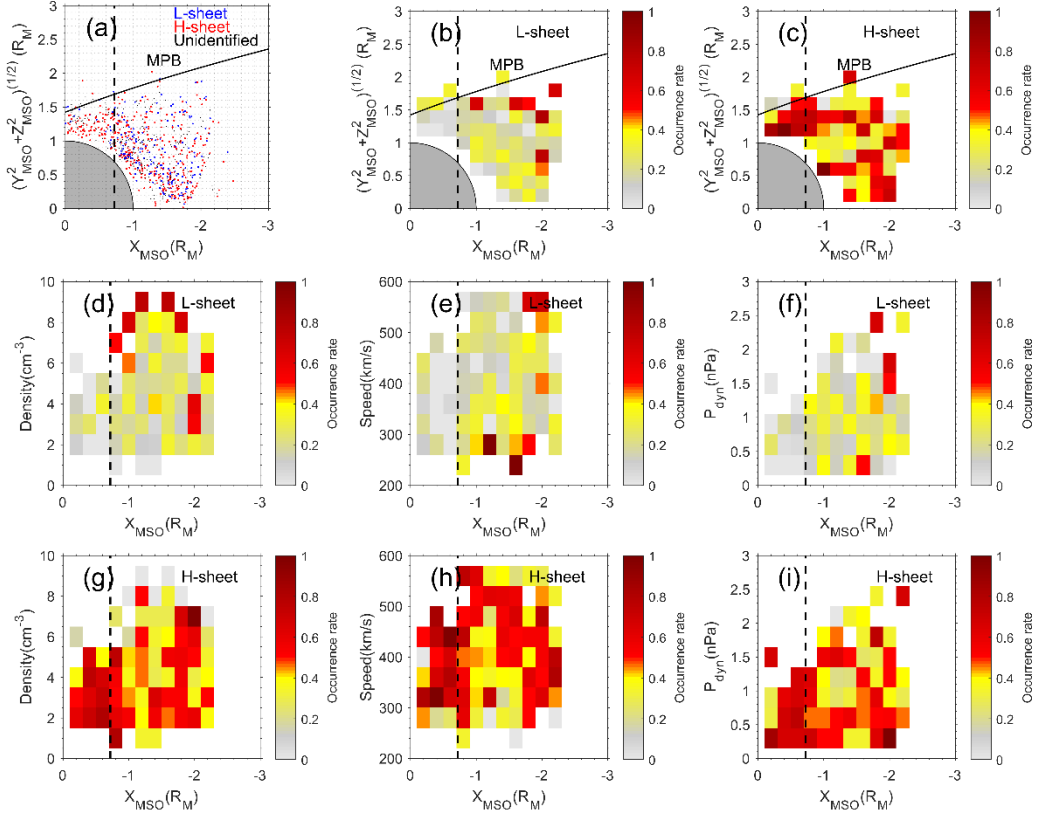


Figure 3. Statistical distributions of surveyed current sheet events. Panels in the top row, from left to right, show the scattering plot of events in cylindrical coordinates in MSO (a), the occurrence rate of the L-sheet (b), and the occurrence rate of the H-sheet (c). Panels in the middle row show the L-sheet

occurrence rate varied with downstream distance and the solar wind proton density (d), dynamic pressure (e), and speed (f), respectively. Similarly, the panels in bottom show the occurrence rate of the H-sheet varied with solar wind proton density (g), dynamic pressure (h), and speed (i), respectively. The vertical dashed line in each panel marks where $X_{MSO}=0.75 R_M$. Note that, to lower the bias, we only keep bins whose number of data points exceeds three.

The L-sheet occurrence rate, which varies against downstream distance (X_{MSO}) and solar wind parameters, demonstrates that the L-sheet seldom occurs when closer to the terminator ($X > -0.75 R_M$) and that it becomes significant beyond $X < -0.75 R_M$ (Figure 3d-3f and Figure S2 in Supporting Information S1). This occurrence rate beyond $X < -0.75 R_M$ weakly increases with solar wind density and dynamic pressure, but is not significantly correlated with solar wind speed (Figure 3d-3f and Figure S3 in Supporting Information S1).

In contrast, the current sheet is almost always an H-sheet, regardless of the solar wind variation, when closer to the terminator ($X > -0.75 R_M$) (Figure 3g-3i). This occurrence rate beyond $X < -0.75 R_M$ shows a weak decrease with solar wind density and dynamic pressure and, like the L-sheet, has no significant correlation with solar wind speed (Figure S3 in Supporting Information S1).

5. Summary and Discussion

Based on the MAVEN measurements of ion density in different species of the Martian tail current sheet, we report, for the first time, that the dominant ion species in surveyed tail current sheets is variable: that is, the current sheet is dominated by either planetary heavy ions or (sometimes) H^+ . Our findings demonstrate that a current sheet closer to the terminator ($X > -0.75 R_M$) is dominated by heavy ions (O^+ and O_2^+) regardless of the variations of solar wind. For a current sheet with a downstream distance beyond $X < -0.75 R_M$, both H^+ and heavy ions are likely to be the dominant ion species, which is more sensitive to variations of upstream solar wind. We find that the occurrence rate of the current sheet with dominant H^+ (heavy ions) weakly increases (decreases) with solar wind density and dynamic pressure but is not significantly correlated with solar wind speed.

One question may naturally arise about the origin of the dominant H^+ because both ionosphere and solar wind could be potential sources. We have preliminarily addressed this issue from two aspects: 1. Since the typical energy of H^+ from the solar wind is higher than tens of eV, we find that cases with H^+ energy higher than 30 eV account for about 75% of the selected L-sheet cases (details are not shown here). 2. In most L-sheet cases, we find the energy flux of He^{++} (He^{++} is from solar wind) also shows enhancement although the energy of detected H^+ sometimes is several tens of eV, e.g. the two cases shown in Figure 2 (not shown here). Thus, the dominant H^+ in the tail current sheet is mostly from the solar wind, nonetheless, the strong deceleration process of H^+

from the solar wind to the tail is unclear yet. One could survey it exclusively by comparison with simulations.

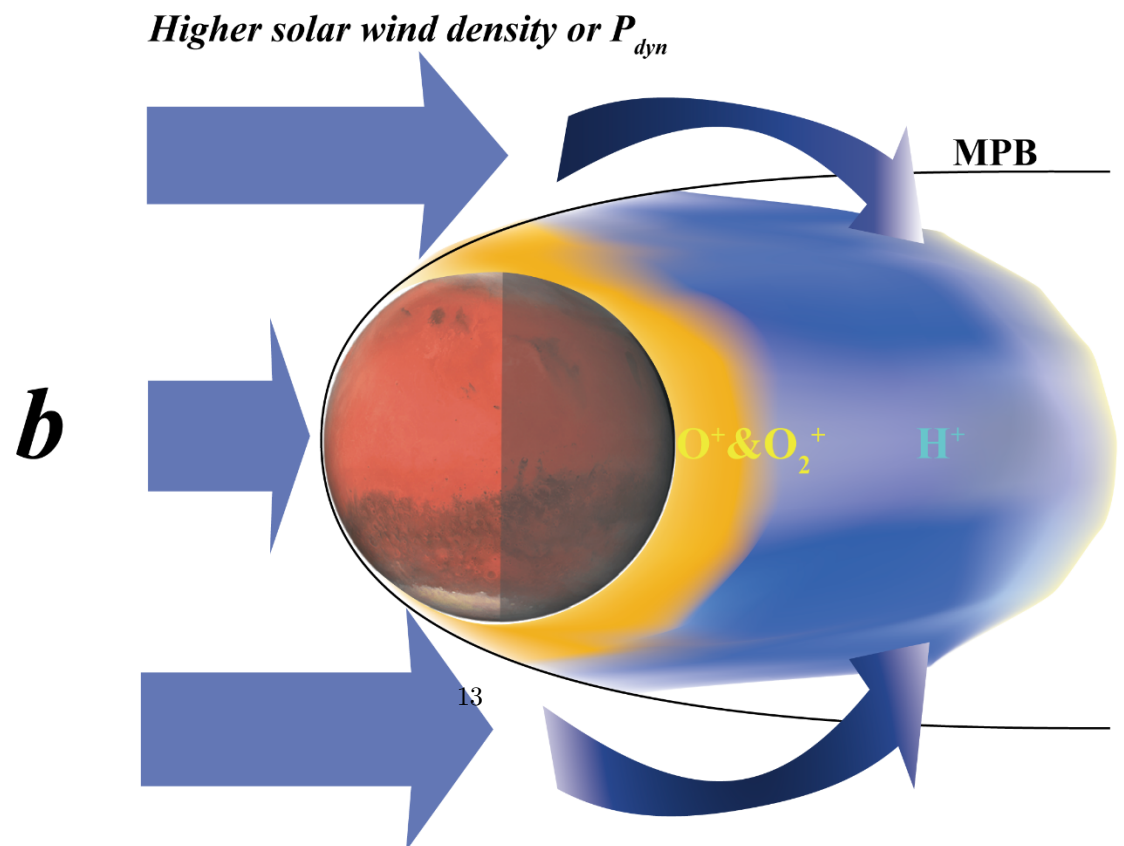
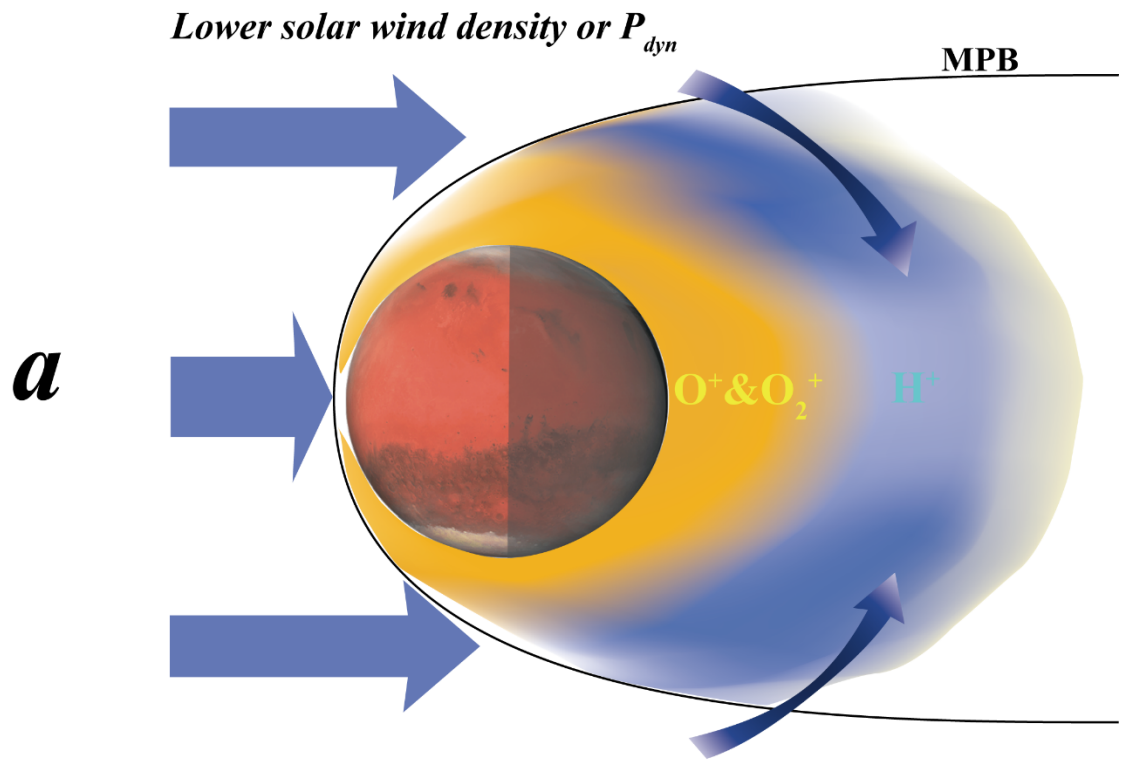


Figure 4. Diagram of the variation of dominant ion species in the Martian tail current sheet under different solar wind conditions. The upper panel shows a case with lower solar wind density or dynamic pressure (a), and the lower panel shows a case with higher solar wind density or dynamic pressure (b).

Our conclusions are plausible because heavy ions in the tail current sheet must originate from the Martian ionosphere, ions that should dominate when current sheets are close to the planet. When the tail is far away from the terminator, the density of heavy ions decreases significantly, and H^+ , mostly from solar wind, could gradually diffuse into the cavity of the tail and quite possibly become the dominant ion species in the current sheet, particularly when the solar wind density or dynamic pressure is higher. We sketched a diagram in Figure 4 to summarize our findings.

However, the factors that account for variation in the dominant ion species cannot be restricted to downstream distance and solar wind. For example, the current sheet shown on the right of Figure 2 has a comparatively higher solar wind density and dynamic pressure, but heavy ions dominate. Thus there might be other factors that control the ion composition. More work is needed to address this issue.

Interestingly, we find the response of the H-sheet or L-sheet occurrence rate to solar wind to be very similar to that of the heavy ion escape rate. Previous studies suggested that the heavy ion escape rate from the tail has a weak inverse dependence on solar wind density and dynamic pressure, and no significant dependence on solar wind velocity [Ramstad et al., 2015; Dubinin et al., 2017; Ramstad et al., 2018]. One reason might be that enhanced solar wind density causes a weak decrease of heavy ion density in the current sheet, which lowers the H-sheet occurrence rate as well as the heavy ion escape rate. However, few know how the density of different ion species in the tail current sheet varies as a response to upstream solar wind (Liu et al., 2021), we wish to survey this question in our next study.

It has to be pointed out that the E-asymmetry of density or flux of heavy ions (e.g. Dubinin et al., 2017, 2019) does not necessarily imply an E-asymmetry of the occurrence of the current sheet type, and we do not find an evident E-asymmetry of the occurrence of H-sheet in MSE (Figure S1c in Supporting Information S1).

It is not clear whether the detected H-sheet or L-sheet is a local or transient structure. Possible collaboration between MAVEN (Jakosky et al., 2015), Mars Express (Barabash et al., 2006), and Tianwen-1 (Wan et al., 2020) may help to ascertain the spatial scale and duration of the sheet of a given type, as well as its response to variations in upstream solar wind.

Data Availability Statement

All MAVEN data used in this paper are available from NASA’s Planetary Data System. MAG data can be found at <https://pds-ppi.igpp.ucla.edu/mission/MAVEN/MAVEN/MAG>.

SWIA data can be found at <https://pds-ppi.igpp.ucla.edu/mission/MAVEN/MAVEN/SWIA>.
SWEA data can be found at <https://pds-ppi.igpp.ucla.edu/mission/MAVEN/MAVEN/SWEA>.

Acknowledgments

We would like to thank the entire MAVEN team and instrument leads for access to data and support. This work is supported by the National Natural Science Foundation of China (Grant Nos. 41922031, 41774188), the Strategic Priority Research Program of Chinese Academy of Sciences (Grant Nos. XDA17010201, XDB41000000), the Key Research Program of Chinese Academy of Sciences (Grant No. ZDBS-SSW-TLC00103), and the Key Research Program of the Institute of Geology & Geophysics, CAS (Grant No. IGGCAS- 201904, IGGCAS-202102).

References

- Acuña, M. H., Connerney, J. E. P., Wasilewski, P., Lin, R. P., Anderson, K. A., Carlson, C. W., McFadden, J., Curtis, D. W., Mitchell, D., et al. (1998). Magnetic field and plasma observations at mars: initial results of the mars global surveyor mission. *Science*, 279(5357), 1676–1680. doi:10.1126/science.279.5357.1676
- Artemyev, A. V., V. Angelopoulos, J. S. Halekas, A. Runov, L. M. Zelenyi, and J. P. McFadden (2017), Mars’s magnetotail: Nature’s current sheet laboratory, *Journal of Geophysical Research: Space Physics*, 122, 5404–5417, doi:10.1002/2017JA024078.
- Barabash, S., et al. (2006), The Analyzer of Space Plasma and Energetic Atoms (ASPERA-3) for the Mars Express mission, *Space Science Review.*, 126, 113.
- Barabash, S., A. Fedorov, R. Lundin, and J.-A. Sauvaud (2007), Martian atmospheric erosion rates, *Science*, 315, 501–503; doi:10.1126/science.1134358.
- Brain, D., et al. (2010), A comparison of global models for the solar wind interaction with Mars, *Icarus*, 206, 139–151, doi:10.1016/j.icarus.2009.06.030
- Carlsson, E. et al. (2006), Mass composition of the escaping plasma at Mars, *Icarus*, 182(2), 320–328, doi:10.1016/j.icarus.2005.09.020
- DiBraccio, G. A., et al. (2015), Magnetotail dynamics at Mars: Initial MAVEN observations, *Geophysical Research Letters*, 42, 8828–8837, doi:10.1002/2015GL065248
- Dubinin, E., & Fraenz, M. (2015). Magnetotails of Mars and Venus. *Geophysical Monograph Series*, 207, 43–59. doi: 10.1002/9781118842324.ch3
- Dubinin, E., Fraenz, M., Pätzold, M., McFadden, J., Halekas, J. S., DiBraccio, G. A., Zelenyi, L. (2017). The effect of solar wind variations on the escape of oxygen ions from Mars through different channels: MAVEN observations. *Journal of Geophysical Research: Space Physics*, 122, 11,285–11,301. doi: 10.1002/2017JA024741

- Dubinin, E., Modolo, R., Fraenz, M., Pätzold, M., Woch, J., Chai, L., et al. (2019). The induced magnetosphere of Mars: Asymmetrical topology of the magnetic field lines. *Geophysical Research Letters*, 46, 12,722–12,730. <https://doi.org/10.1029/2019GL084387>
- Dubinin, E., Fraenz, M., Pätzold, M., Tellmann, S., Woch, J., McFadden, J., & Zelenyi, L. (2021). Bursty ion escape fluxes at Mars. *Journal of Geophysical Research: Space Physics*, 126, e2020JA028920. doi:10.1029/2020JA028920
- Eastwood, J. P., D. A. Brain, J. S. Halekas, J. F. Drake, T. D. Phan, M. Øieroset, D. L. Mitchell, R. P. Lin, and M. Acuña (2008), Evidence for collisionless magnetic reconnection at Mars, *Geophysical Research Letters*, 35, L02106, doi:10.1029/2007GL032289.
- Fang, X., M. W. Liemohn, A. F. Nagy, J. G. Luhmann, and Y. Ma (2010), On the effect of the Martian crustal magnetic field on atmospheric erosion, *Icarus*, 206, 130; doi: 10.1016/j. icarus.2009.01.012.
- Fedorov, A., et al. (2008), Comparative analysis of Venus and Mars magnetotails, *Planet. Space Sci.*, 56, 812–817, doi: 10.1016/j.pss.2007.12.012.
- Gao, J.W., Rong, Z.J., Klinger Lucy, Li, X.Z., Liu, D., Wei, Y. (2021). A spherical harmonic Martian crustal magnetic field model combining data sets of MAVEN and MGS, *Earth and Space Science*, doi: 10.1029/2021EA001860.
- Harada, Y., et al. (2015), Magnetic reconnection in the near-Mars magnetotail: MAVEN observations, *Geophysical Research Letters*, 42, 8838–8845, doi:10.1002/2015GL065004
- Harada, Y., et al. (2017), Survey of magnetic reconnection signatures in the Martian magnetotail with MAVEN, *Journal of Geophysical Research: Space Physics*, 122, 5114–5131, doi:10.1002/2017JA023952.
- Halekas, J. S., D. A. Brain, R. J. Lillis, M. O. Fillingim, D. L. Mitchell, and R. P. Lin (2006), Current sheets at low altitudes in the Martian magnetotail, *Geophysical Research Letters*., 33, L13101, doi:10.1029/2006GL026229.
- Halekas, J. S., J. P. Eastwood, D. A. Brain, T. D. Phan, M. Øieroset, and R. P. Lin (2009), In situ observations of reconnection Hall magnetic fields at Mars: Evidence for ion diffusion region encounters, *Journal of Geophysical Research: Space Physics*., 114, A11204, doi:10.1029/2009JA014544
- Inui, S., Seki, K., Sakai, S., Brain, D. A., Hara, T., McFadden, J. P., et al. (2019). Statistical study of heavy ion outflows from Mars observed in the Martian-induced magnetotail by MAVEN. *Journal of Geophysical Research: Space Physics*, 124, 5482–5497. <https://doi.org/10.1029/2018JA026452>
- Jakosky, B. M., Lin, R. P., Grebowsky, J. M., Luhmann, J. G., Mitchell, D. F., Beutelschies, G., Priser, T., Acuna, M., Andersson, L., et al. (2015). The Mars Atmosphere and Volatile Evolution (MAVEN) mission. *Space Science Review*., 195(1), 3–48. <https://doi.org/10.1007/s11214-015-0139-x>

- Liemohn, M.W. and Xu, S. (2018). Recent Advances Regarding the Mars Magnetotail Current Sheet. In *Electric Currents in Geospace and Beyond* (eds A. Keiling, O. Marghitu and M. Wheatland). doi:10.1002/9781119324522.ch11
- Liu, D., Rong, Z., Gao, J., He, J., Klinger, L., Dunlop, M. W., et al. (2021). Statistical properties of solar wind upstream of Mars: MAVEN observations. *The Astrophysical Journal*, 911(2), 113. doi:10.3847/1538-4357/abed50
- Lundin, R., Barabash, S., Futaana, Y., Sauvaud, J.-A., Fedorov, A., Perez-de-Tejada, H., (2011), Ion flow and momentum transfer in the Venus plasma environment, *Icarus*, Volume 215, Issue 2, , Pages 751-758, ISSN 0019-1035, doi:10.1016/j.icarus.2011.06.034.
- Luhmann, J. G., and L. H. Brace (1991), Near-Mars space, *Rev. Geophys.*, 29, 121–140.
- Ma, Y., A. F. Nagy, K. C. Hansen, D. L. DeZeeuw, and T. I. Gombosi (2002), Three-dimensional multispecies MHD studies of the solar wind interaction with Mars in the presence of crustal fields, *Journal of Geophysical Research: Space Physics.*, 107(A10), 1282; doi: 10.1029/2002JA009293.
- Ma, Y. J., et al. (2015), MHD model results of solar wind interaction with Mars and comparison with MAVEN plasma observations, *Geophysical Research Letters.*, 42, 9113–9120, doi:10.1002/2015GL065218
- Maes, L., Fraenz, M., McFadden, J. P., & Benna, M. (2021). Escape of CO₂ + and other heavy minor ions from the ionosphere of Mars. *Journal of Geophysical Research: Space Physics*, 126, e2020JA028608. <https://doi.org/10.1029/2020JA028608>
- McComas, D. J., H. E. Spence, C. T. Russell, and M. A. Saunders (1986), Magnetic field draping and consistent plasma properties of the Venus magnetotail, *Journal of Geophysical Research: Space Physics.*, 91, 7939–7953.
- Najib, D., A. F. Nagy, G. Tóth, and Y. Ma (2011), Three-dimensional, multifluid, high spatial resolution MHD model studies of the solar wind interaction with Mars, *Journal of Geophysical Research: Space Physics.*, 116, A05204; doi:10.1029/2010JA016272.
- Ramstad, R., S. Barabash, Y. Futaana, H. Nilsson, X.-D. Wang, M. Holmström, The Martian atmospheric ion escape rate dependence on solar wind and solar EUV conditions: 1. Seven years of Mars Express observations. *Journal of Geophysical Research: Planets* 120, 1298–1309 (2015). doi: 10.1002/2015JE004816
- Ramstad, R., S. Barabash, Y. Futaana, H. Nilsson, M. Holmström, Ion escape from Mars through time: An extrapolation of atmospheric loss based on 10 years of Mars Express measurements. *Journal of Geophysical Research: Planets* 123, 3051–3060 (2018). <https://doi.org/10.1029/2018JE005727>
- Trotignon, J.G.; Mazelle, C.; Bertucci, C.; Acuña, M.H. (2006). Martian shock and magnetic pile-up boundary positions and shapes determined from the Pho-

bos 2 and Mars Global Surveyor data sets, *Planetary and Space Science* 54(4), 357–369. doi:10.1016/j.pss.2006.01.003

Verscharen, D., Klein, K.G. & Maruca, B.A. The multi-scale nature of the solar wind. *Living Rev Sol Phys* 16, 5 (2019). doi:10.1007/s41116-019-0021-0

Wan, W. X., Wang, C., Li, C. L., Wei, Y., and Liu, J. J. (2020). The payloads of planetary physics research onboard China's First Mars Mission (Tianwen-1). *Earth and Planet Physics.*, 4(4), 331–332. doi:10.26464/epp2020052

Xu, S., M. W. Liemohn, C. Dong, D. L. Mitchell, and S. M. Bougher (2016), Pressure and ion composition boundaries at Mars, *Journal of Geophysical Research: Space Physics*, 121, 6417–6429; doi: 10.1002/2016JA022644.

Zhang, C., Rong, Z., Nilsson, H., Klinger, L., Xu, S., Futaana, Y., et al. (2021). MAVEN observations of periodic low-altitude plasma clouds at Mars. *The Astrophysical Journal Letters*, 922(2), L33. <https://doi.org/10.3847/2041-8213/ac3a7d>

Zhang, C., Rong, Z., Klinger, L., Nilsson, H., Shi, Z., He, F., et al. (2022). Three-dimensional configuration of induced magnetic fields around Mars. *Journal of Geophysical Research: Planets*, 127, e2022JE007334. <https://doi.org/10.1029/2022JE007334>